

Polymer Chemistry

Accepted Manuscript



This is an *Accepted Manuscript*, which has been through the Royal Society of Chemistry peer review process and has been accepted for publication.

Accepted Manuscripts are published online shortly after acceptance, before technical editing, formatting and proof reading. Using this free service, authors can make their results available to the community, in citable form, before we publish the edited article. We will replace this *Accepted Manuscript* with the edited and formatted *Advance Article* as soon as it is available.

You can find more information about *Accepted Manuscripts* in the [Information for Authors](#).

Please note that technical editing may introduce minor changes to the text and/or graphics, which may alter content. The journal's standard [Terms & Conditions](#) and the [Ethical guidelines](#) still apply. In no event shall the Royal Society of Chemistry be held responsible for any errors or omissions in this *Accepted Manuscript* or any consequences arising from the use of any information it contains.

High Strain Epoxy Shape Memory Polymer

Ning Zheng[†], Guangqiang Fang^{‡, §}, Zhengli Cao[§], Qian Zhao[†], Tao Xie^{†*}

[†]State Key Laboratory of Chemical Engineering, College of Chemical and Biological Engineering, Zhejiang University, 38 Zheda Road, Hangzhou, 310027, P. R. China

[‡]State Key Laboratory of Metal Matrix Composites, School of Materials Science and Engineering, Shanghai Jiaotong University, 800 Dongchuan Road, Shanghai, 200240, P. R. China

[§]Aerospace System Engineering Shanghai, 3805 Jindu Road, Shanghai, 201108, P. R. China

ABSTRACT: Epoxy polymers represent a recently emerged class of thermoset shape memory polymers with superior thermo-mechanical endurance and excellent processability. However, the strains at break are typically low for epoxy shape memory polymers. This severely limits their potential applications. In this article, we report a two component epoxy-amine shape memory polymer system with tunable T_g (between 40 °C and 80 °C) and excellent shape memory properties in terms of shape fixity, shape recovery ratios, and cycling stability. Importantly, its values of strain at break above T_g and at the T_g peak reach 111% and 212%, respectively. We anticipate that such a high strain epoxy system will significantly broaden the opportunities for shape memory device applications.

KEYWORDS: Shape Memory Polymer, Epoxy Polymer, Strain at Break

1. INTRODUCTION

Shape memory polymers (SMPs), which are capable of memorizing temporary shapes and recovering to their original forms upon external stimulations, have been highly attractive to the scientific community.¹⁻⁸ The recovery can be triggered by heat,⁹⁻¹⁰ light,¹⁰⁻¹³ electric current,¹⁴⁻¹⁵ magnetic fields,¹⁶ moisture,¹⁷⁻¹⁸ or radiofrequency waves.¹⁹ Despite the diversity of triggering stimuli, heat (either directly or indirectly applied) remains the overwhelmingly popular stimulus for actuating SMPs. Thus, the shape memory transition temperature (T_{trans} , typically T_g or T_m) is one of the most critical parameters for an SMP.²⁰ Recent advances in the SMP field have led to the emergence of a variety of new and exciting applications, including biomedical devices,²¹⁻²³ biomimetic reversible adhesives²⁴⁻²⁶ and programmable optical devices,²⁷⁻²⁸ to name just a few. Besides the shape memory transition temperature, each application typically demands an SMP with a particular set of properties such as biodegradability, strain at break (ϵ_b), or maximum recovery stress (σ_{max}). Amongst all these performance parameters, T_{trans} and ϵ_b are particularly of general relevance.

Thus far, a wide variety of polymers (both thermoplastic and thermoset) have been found with shape memory properties. Many thermoplastic SMPs possess large ϵ_b s,²¹ but their shape recovery is often time less than ideal (with some exceptions^{9, 29}). In contrast, thermoset SMPs typically exhibit excellent shape fixing and recovery behaviors. Thermoset SMPs can be created by either introducing crosslinking in thermoplastic polymers or direct curing of liquid monomers with crosslinkers. The latter has two notable advantages over the former: more flexible structural tuning

through comonomer and crosslinker selections, and easier processing into complex devices owing to the liquid nature of the precursors. Because of these, thermoset SMPs obtained from direct curing of liquid precursors have become the focus of many studies. This type of thermoset SMPs include (meth)acrylate-based systems,³⁰⁻³² thiol-ene systems³³⁻³⁴ and epoxy-based systems.³⁵⁻⁴² For (meth)acrylate-based systems, its ϵ_b can be tuned to an extremely high level while still maintaining high shape fixity and shape recovery.³¹ This type of system, however, often time suffer from several processing issues: the volatility of some (meth)acrylate monomers, high curing shrinkage, and oxygen inhibition during curing. Amongst them, the high curing shrinkage is particularly cumbersome to deal with if devices with high precision microstructures are to be produced. Thiol-ene systems,³³⁻³⁴ on the other hand, exhibit much lower volume shrinkage and their curing is not inhibited by oxygen. However, the values of ϵ_b for thiol-ene systems are not typically reported in the literature.

Epoxy SMPs have gained significant attention lately. Its increasing popularity stems from many attributes including the versatility of the curing chemistry, the availability of a wide variety of non-volatile monomers, the low curing shrinkage, and the excellent thermo-mechanical stability of the cured polymers.^{20,35-41} This has led to epoxy SMPs with highly tunable T_g s.²⁰ Of equal importance is that they can also be easily processed into attractive SMP devices^{25, 43-44} as well as self-healing systems^{45,46} and triple-shape composites.^{47,48} Despite the advantages of epoxy SMPs, they typically suffer from low ϵ_b values. A prototypical example of an epoxy SMP system²⁰ was obtained by curing between an aliphatic diamine and a mixture of an aromatic

diepoxide and an aliphatic diepoxide. While maintaining the overall stoichiometry between the amine and epoxy functional groups, a series of SMPs were obtained by changing the ratio between the rigid aromatic diepoxy and the flexible aliphatic diepoxide in the formulations. This allowed adjusting the overall network flexibility, thus arbitrary tuning of the T_g in a wide temperature range between 25 °C and 100 °C. However, the ϵ_b values for such an epoxy system were no greater than 30% due to the inherent high crosslinking densities. Although various low strain SMP applications have recently emerged, it is highly desirable to extend epoxy SMP systems to a much higher ϵ_b range to fully take advantage of their easy processability for a much wider range of applications. A physical strategy to increase the ϵ_b of a particular SMP material as pioneered by Gall's group was to deform it around the onset of the T_g transition, instead of above its T_g .⁴⁹ This strategy was adopted by Rousseau et al for an epoxy SMP and its ϵ_b was indeed improved from 30% to ca. 60%.³⁵ However, shape fixity ratios were noticeably compromised under such conditions, which may not be acceptable for many applications. Thus, improving ϵ_b s for epoxy SMPs without compromising shape fixing performance is highly desirable. One such an effort was reported by Leng et al, which claimed a high strain epoxy SMP system.³⁸ Unfortunately, the detailed SMP formulations were not revealed except that it was known to be a three component system with an epoxy base resin, a hardener, and a linear epoxy monomer. Leonardi et al, by contrast, reported the detailed formulation of an epoxy SMP system composed of an aromatic diepoxide, a long-chain monoamine, and an aromatic diamine as the crosslinking agent.³⁹ The cured network comprises of chemical crosslinking and

intriguing physical crosslinking owing to the tail-to-tail association of the long alkyl chains. ϵ_b as high as 75% was achieved, but only for one single formulation with a T_g around 40 °C. This example nevertheless represents the current state of art of high strain epoxy SMP with a precisely known chemical composition. With the practical need for T_g tunable epoxy SMPs with even higher ϵ_b , we set to develop epoxy SMPs using most commonly available commercial epoxy components. This effort was reported hereafter in this paper.

2. EXPERIMENTAL SECTION

2.1. Materials. The epoxy monomer E44 (molecular weight ~450 g/mol and epoxy equivalent weight 210~240 g/mol) was purchased from China Petrochemical Corporation. The curing agent poly(propylene glycol)bis(2-aminopropyl)ether (Jeffamine D230, abbreviated as D230 hereafter) was purchased from Sigma-Aldrich. All chemicals were used as received.

2.2. Sample Preparation. In a typical curing experiment, E44 was weighed into a glass bottle and melted by heating in an oven at 60 °C. Afterwards, weighed Jeffamine D-230 was added into the bottle, which was vigorously shaken by hand for complete mixing. The mixture was poured into an aluminum pan. Curing was conducted thermally at 100 °C for 1h followed by a postcure at 130 °C for 1h. Finally, the cured sample was demolded and cut into dog bones with a laser cutter for further testing.

2.3. Thermal analyses. Differential scanning calorimetry (DSC) measurements were conducted using DSC Q200 (TA instruments) at a cooling and heating rate of

10 °C/min. Dynamic mechanical (DMA) analyses were conducted using DMA Q800 (TA instruments). The conditions for the DMA experiments were: tensile, “multi-frequency, strain” mode at 1 Hz, 0.2% strain, and a heating rate of 3 °C /min. Samples of 1 mm thickness and 2.5 mm width were used.

2.4. Shape memory properties. For qualitative shape memory demonstrations, samples of rectangular shapes (1×5×2.5mm) were used. In a typical experiment, the sample was first immersed in a water bath preset above its T_g for 5 s. It was then taken out of the bath and immediately deformed into a temporary shape. With the deformation force maintained on the sample, it was cooled at room temperature. Subsequent release of the deformation force after cooling completed the shape fixing step. Shape recovery was accomplished by immersing the deformed sample into the same water bath.

Quantitative shape memory performance was evaluated using DMA Q800 in a "controlled force" mode. The heating rate and cooling rate were 10 °C /min and the 5 °C /min, respectively. The shape fixity (R_f) and shape recovery (R_r) were calculated using the following equations as defined in Ref.¹

$$R_f = \varepsilon_d / \varepsilon_{dload} \quad \text{and} \quad R_r = (\varepsilon_d - \varepsilon_{rec}) / \varepsilon_d,$$

where ε_{dload} and ε_{rec} respectively represent the maximum strain under load and the recovered strain, and ε_d is the fixed strain after cooling and load removal.

2.5. Measurements of strains at break (ε_b s). ε_b values were measured using a universal material testing machine (Zwick/Roell Z005) equipped with a thermal chamber. The experiments were conducted in a tensile mode at a crosshead speed of 10

mm/min and a heating rate of 20 °C /min. ϵ_b was typically recorded as the maximum strain prior to the sample break at its rubbery state. Samples in dog bone shapes with the neck dimensions of 1.2×4.5 mm were used. At least five specimens were tested for each sample to obtain statistically meaningful data.

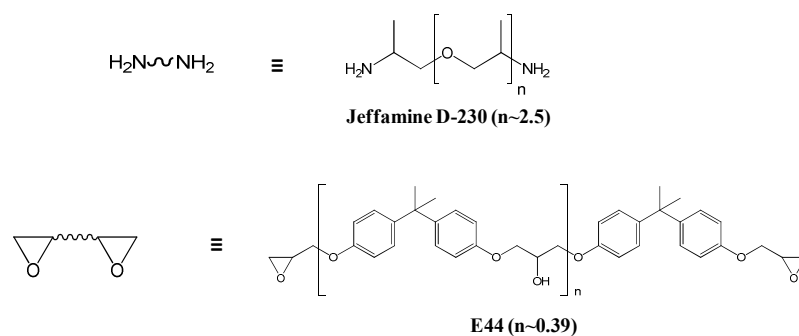
3. RESULTS AND DISCUSSION

A rule of thumb to increase the ϵ_b of an amorphous thermoset SMP is to reduce the crosslinking density whereas T_g is affected by both the crosslinking density and the chain flexibility. Such a design principle has been applied quite successfully to (meth)acrylate SMPs.³⁰⁻³² Whereas the rule may also be applicable to epoxy SMPs, there appear to be additional factors that should be considered. For instance, we reported a thermoset epoxy SMP system based on the curing between an aromatic diepoxide and an aliphatic diamine. Replacing the aliphatic diamine with a mono-amine (decylamine) while maintaining the overall stoichiometric balance between the amine and the epoxide led to a series of SMPs with tunable T_g s.²⁰ However, the SMPs with more decylamine (thus lower crosslinking densities) in the formulation did not show noticeable improvement on ϵ_b . An intriguing comparison can be made with the high strain example mentioned in the introduction in which the epoxy system was obtained by curing *n*-dodecylamine, an aromatic diamine crosslinker, and an aromatic diepoxide.³⁹ The formulations in these two examples appear quite similar, yet the outcome in terms of ϵ_b is drastically different. This emphasizes the network design in which the former network simply has dangling

decyl chains²⁰ whereas the longer dodecyl chains in the latter³⁹ possess the tail-to-tail association that is apparently important. With all these considerations in mind, we herein aimed to simplify the epoxy network design to achieve tunable crosslinking density without involving the potentially non-beneficial dangling chains. Our network design started with a previously reported base epoxy SMP formulation obtained by curing an aromatic diepoxide (EPON 826 with an epoxy equivalent weight of 180) and an aliphatic diamine (D230).²⁰ This particular SMP has a T_g around 100 °C and ϵ_b below 30% owing to its high crosslinking density. Two approaches were combined to reduce the crosslinking density. First, EPON 826 was replaced by another diepoxide (E44) with a much higher epoxy equivalent weight of 225 (Figure 1). Second, while we still employed the same D230 (also in Figure 1) as the crosslinker, the ratio between E44 and D230 was shifted away from their stoichiometry with the D230 in excess. This led to the network structure in Figure 1, in which some of the hydrogen atoms on NH groups remain unreacted. This conceptual structure is based on the assumption that primary amine hydrogens are preferentially consumed due to their higher reactivity than secondary amine hydrogens.⁵⁰⁻⁵² Thus, this would statistically leave unreacted hydrogens mostly in the secondary amino form. We further note that actual reaction and gelation is highly complex in crosslinked systems. It is outside the scope of the current study to investigate such aspects and we simply use the somewhat idealized structure in Figure 1 for qualitative guidance only. In its stoichiometric state, each hydrogen atom on the amine group serves as a crosslinking site. Thus, the excess amines in the formulation left unreacted amine hydrogens that led to the reduction of

the network crosslinking density. An additional important consideration here is that, after full curing with the epoxy groups in the formulation, the remaining unreacted amino hydrogens are not expected to undergo additional reactions under conditions SMPs are typically used. This is necessary for the durability of the SMPs.

Epoxy precursors



Epoxy networks

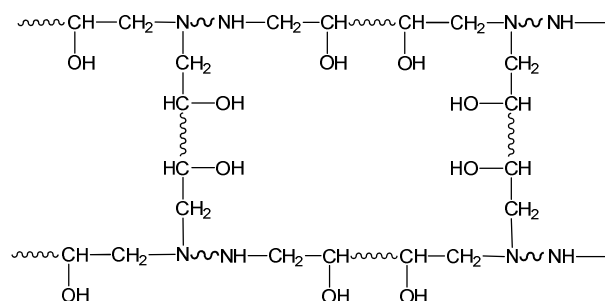


Figure 1. Chemical structures of the epoxy precursors and cured networks.

Accordingly, four epoxy samples (**Epon1** to **Epon4** in Table 1) were prepared by varying the ratio between E44 and D230. The crosslinking density for each sample, which can be calculated (equation 1) based on its rubbery modulus reported later in the context (Figure 5), is included in Table 1.

$$d = \frac{E_r}{3RT} \quad \text{Eq. (1)}$$

where d represents the crosslinking density per unit volume (mol/cm^3), E_r is rubbery modulus (MPa), R and T are the gas constant and the absolute temperature, respectively.

Table 1 Compositions and shape memory performances of the epoxy samples.

Samples	E44 (mol)	D230 (mol)	d ($10^{-3}\text{g}/\text{mol}$)	R_f (%)	R_r (%)
Epon1	1	1	2.3	99.8	98.1
Epon2	1.33	1	3.5	99.5	97.4
Epon3	1.67	1	6.1	99.4	98.2
Epon4	2	1	6.3	99.5	99.4

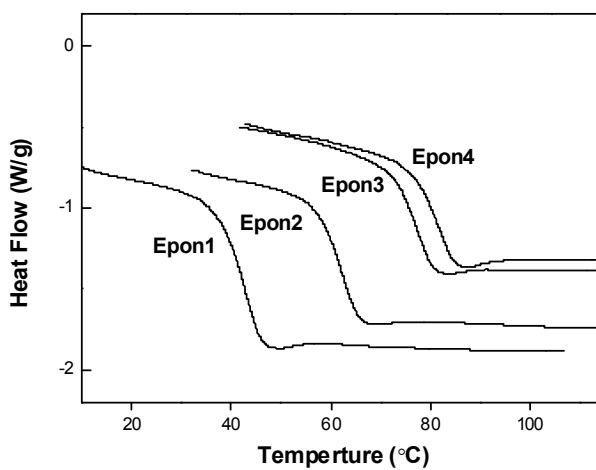


Figure 2. DSC curves of the epoxy samples.

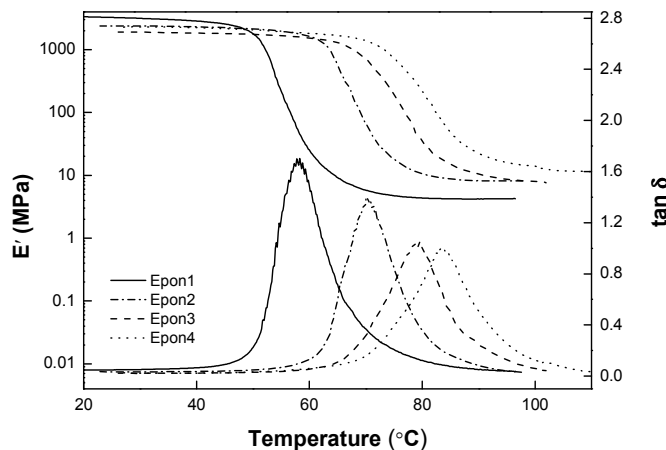


Figure 3. DMA curves of the epoxy samples.

As the ratio between D230 and E44 increases from **Epon1** to **Epon4**, the crosslink density goes up dramatically. Attempts were also made to prepare a sample with the molarity ratio of 0.98 (between E44 and D230). This sample failed to cure into a solid, implying that **Epon1** had already approached the lowest achievable crosslinking density for the current two component epoxy system. The DSC curves of the cured epoxy samples are shown in Figure 2. All the samples showed readily observable T_g transitions between 40 °C and 80 °C, with increasing T_g from **Epon1** to **Epon4**. DMA curves for these samples (Figure 3) show the same trend except that the T_g transitions appear to be higher, as judged from their respective temperature corresponding to the $\tan\delta$ peaks. Closer examination of the DMA curves in Figure 3 revealed that all the samples show relatively constant storage modulus in their glass state. Importantly, they all possess nice and flat rubbery plateau, a good indication of their crosslinked nature and their potential shape memory functions. The rubbery modulus increases from **Epon1** to **Epon4**, which is consistent with the increasing crosslinking density. The T_g 's obtained from DSC and DMA are quantitatively compared in Figure 4. The T_g and

the molar ratio between E44 and D230 show an almost linear relationship at molar ratios below 1.67. Above this ratio, the slope of the T_g increase appears to decrease, indicating that when the crosslink density reaches a specific value, the change in the formulation has less impact on the T_g . Overall, the continuous change of the T_g with the molar ratio suggests that any T_g in these temperature ranges can be obtained.

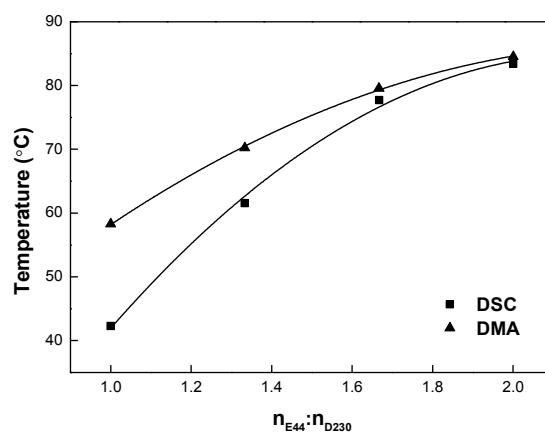


Figure 4. Glass transition temperatures of the epoxy samples.

The ϵ_b and E_r (rubbery modulus) values for the different samples, as measured using a tensile tester, are summarized in Figure 5. **Epon4**, with the molar ratio of 2 between E44 and D230, shows a low ϵ_b around 40% and a high E_r of 14 MPa. This is not surprising due to the high crosslinking nature. **Epon3**, which has a lower molar ratio of 1.67 between E44 and D230, has similar ϵ_b and E_r values. This appears to be consistent with the T_g trend shown in Figure 4, that is, the change in the molar ratio from 2 to 1.67 does not seem to impact much the material property. Below the molar ratio of 1.67, however, the ϵ_b value significantly increases with the decrease of the molar ratio and E_r follows an opposite trend. Impressively, **Epon1**, with the lowest crosslink density and lowest E_r of 2.1 MPa, reaches the highest ϵ_b value of 111%. Here

in Figure 5, the ϵ_b value for each sample was obtained above its T_g , i.e., at a temperature in the rubbery plateau region. It is known in the literature that ϵ_b values can be positively impacted by deforming an SMP within the glass transition.^{36,39} With this in mind, **Epon1** was subjected to uniaxial tests at different temperatures around its T_g transition and the obtained stress strain curves are shown in Figure 6. As can be seen from this figure, the ϵ_b value indeed increased when the test temperature decreased. Impressively, the ϵ_b value when tested at 50 °C reached 212% (average over five tests).

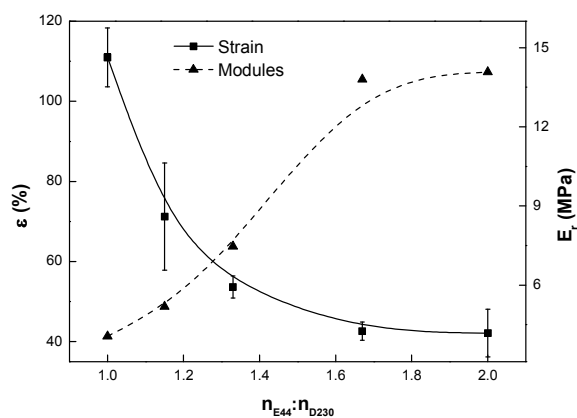


Figure 5. ϵ_b and E_r of the epoxy SMPs

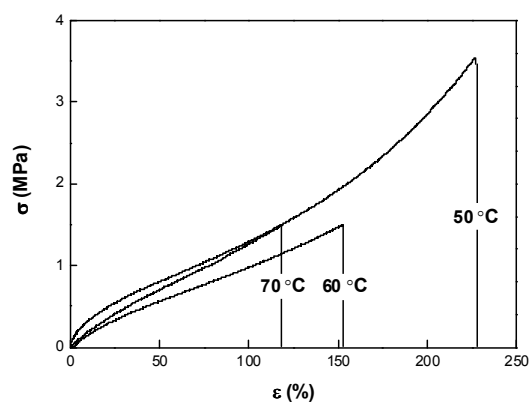


Figure 6. Typical uniaxial stress-strain curves at different temperatures for **Epon1**.

The fact that the epoxy samples all display T_g transitions and rubbery plateaus in their DMA curves indicates that they should possess shape memory behaviors. Qualitatively, a visual demonstration of their shape memory performance is illustrated in Figure 7. Samples from **Epon1** to **Epon4** (in rectangular original shapes) were arranged in such an order in Figure 7a. They were deformed above their respective T_g 's into twisted temporary shapes. Next, immersing in a 60 °C water bath, **Epon1** recovered in 5 seconds (Figure 6c). **Epon2** recovered until the temperature of the water bath rose above 70 °C. As the temperature further increased to 80 °C, **Epon3** recovered in 5 seconds and **Epon4** also recovered at this temperature albeit requiring a longer immersion time of 20 seconds. The shape memory performances of all the samples were further evaluated quantitatively and the results are summarized in Table 1. As can be seen, all the samples show R_f above 99% and R_r above 97%. The quantitative shape memory cycle for a representative sample **Epon1** (with the largest ϵ_b) is plotted in Figure 7, showing near perfect shape fixing ($R_f > 99\%$) and recovery ($R_r > 98\%$) behaviors, despite its very low crosslinking density.

Whereas Figure 7 shows the excellent shape fixity and shape recovery, its high strain capability is difficult to demonstrate with a DMA tester due to the upper limit of the sample displacement within the instrument. A ϵ_b value, on the other hand, is not necessarily equivalent to a maximum recoverable strain even though these two terms are often used interchangeable in the literature. The differences between the two are: 1. it is difficult to approach the ϵ_b in an actual shape memory test without the risk of breaking the sample; 2. shape fixity may not be close to 100% under conditions the

highest ϵ_b value is observed. With these considerations in mind, a separate quantitative shape memory cycle test involving a very high strain was run without using a DMA tester. The experiments were shown in Figure 9. **Epon1** in a dog bone shape was marked by two black lines (distance: 1.5 cm) between the necks. The sample was stretched at 50 °C and the stretching was fixed by cooling. The distance between the two black lines became 4.2cm, corresponding to a strain of ca. 180%. Importantly, this strain can be fully recovered after reheating. The strain of 180% thus represents the highest recoverable strain achieved for **Epon1**, even though theoretically it may be possible to obtain values closer to its ϵ_b of 212%.

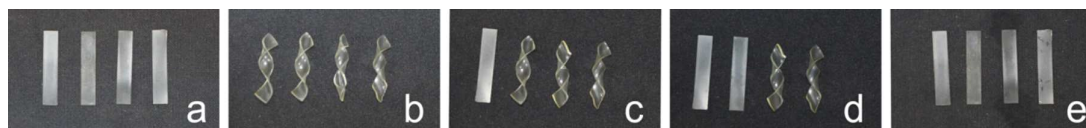


Figure 7. Visual demonstration of shape memory performance of all the epoxy samples (from **Epon1** to **Epon4**). **a**: original shapes; **b**: fixed temporary shapes; **c**: T=60 °C, **Epon1** recovered; **d**: T=70 °C, **Epon2** recovered; **e**: T=80 °C, recovered shapes for all the samples.

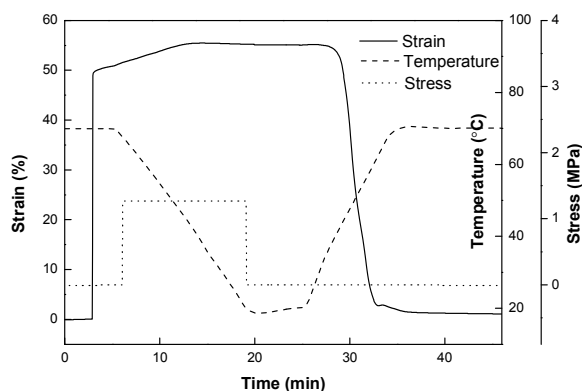


Figure 8. Shape memory cycle for **Epon1**.

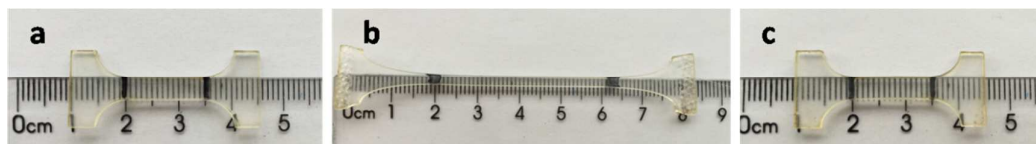


Figure 9. Demonstration of the high strain shape memory performance for **Epon1**.

To investigate the cycling stability of the high strain epoxy SMP, **Epon1** was subjected to consecutive shape memory cycles with the strain above 70%. As shown in Figure 10, the cycle to cycle performance appears to be highly consistent and reproducible with only a slight deviation of the maximum strain from 75.8% to 74.8% after seven cycles. This suggests that, despite the very low crosslinking density, the polymer does possess a homogeneous and robust network.

The advantages of the high strain shape memory performance of **Epon1** are illustrated in Figure 11. In one case, a sample was molded into an original tight spiral, which could be straightened into a temporary shape and recovered to the original one (Figure 11a). Here, the liquid nature of the precursors permitted the use of a liquid molding technique using a simple twisted rubber tube as the mold to make the sophisticated shape (i.e. the spiral). In a second case, a square sample could be tightly folded once in the center line, folded the second time in the perpendicular center line, and folded the third time (Figure 11b). Figure 11c shows the folding steps of the square sample. In this latter case, the temporary shapes involved large strains, yet no fracture was observed and the samples could be completely recovered. These experiments and the experiments in Figure 7 were repeated again 2 months later and no obvious difference in shape memory performance was observed. This confirms the

durability of the current SMP system, at least within the timescale of the investigation.

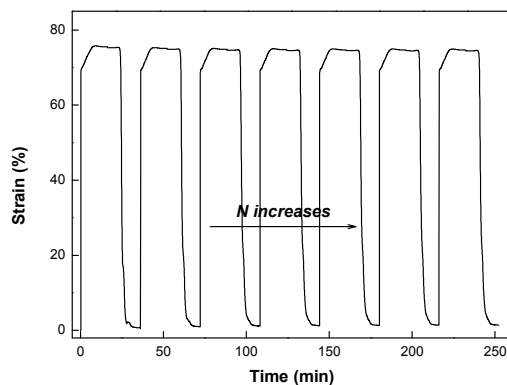


Figure 10. Consecutive shape memory cycles for **Epon1**.

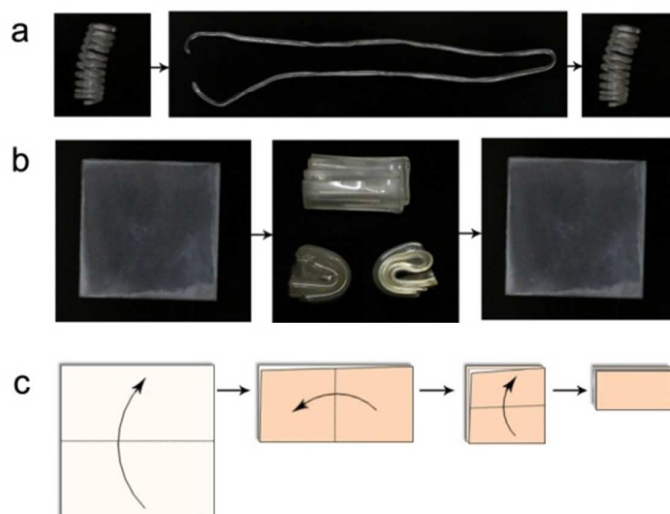


Figure 11. Visual demonstration of the high strain capability for **Epon1**. (a: the shape memory and recovery steps of a tight spiral; b: a square sample was folded three times and visualized in different directions; c: the folding steps of the square sample.)

4. CONCLUSION

A two component epoxy SMP system was developed via the curing between an aromatic diepoxide and an aliphatic diamine. By varying the molar ratio between the two components, the crosslink density and the glass transition temperature (from 40 °C to 80 °C) can be tuned. This led to a high strain epoxy SMP with ϵ_b values of 110% (70 °C, above its T_g) and 212% (50 °C, within its T_g transition). A recoverable strain of 180% can be achieved with this epoxy SMP. In addition to its high strain capability, the SMP also shows excellent shape fixity, shape recovery, and cycling stability. The robustness of the material makes it an ideal candidate for potential SMP device applications.

AUTHOR INFORMATION

Corresponding Author

*Email: taoxie@zju.edu.cn

ACKNOWLEDGEMENTS

We would like to thank the financial support from the following programs: the National Key Basic Research Program of China (Grant No. 2015CB351903), National Natural Science Foundation of China (Grant No. 21474084); the Chinese central government's Recruitment Program of Global Experts; and the 985 program for the startup funding.

REFERENCES

- (1) Xie, T. Recent Advances in Polymer Shape Memory. *Polymer* 2011, 52, 4985-5000.
- (2) Hu, J. L.; Zhu, Y.; Huang, H. H.; Lu, J. Recent Advances in Shape-Memory Polymers: Structure, Mechanism, Functionality, Modeling and Applications. *Prog. Polym. Sci.* 2012, 37, 1720-1763.
- (3) Mather P T.; Luo X.; Rousseau I A. Shape memory polymer research. *Annu. Rev. Mater. Res.* 2009, 39: 445-471.
- (4) Behl, M.; Razaq, M. Y.; Lendlein, A. Multifunctional Shape-Memory Polymers. *Adv. Mater.* 2010, 22, 3388-3410.
- (5) Leng, J. S.; Lan, X.; Liu, Y. J.; Du, S. Y. Shape-Memory Polymers and Their Composites: Stimulus Methods and Applications. *Prog. Mater. Sci.* 2011, 56, 1077-1135.
- (6) Sun, L.; Huang, W. M.; Ding, Z.; Zhao, Y.; Wang, C. C.; Purnawali, H.; Tang, C. Stimulus-Responsive Shape Memory Materials: A Review. *Mater. Des.* 2012, 33, 577-640.
- (7) Lee, K. M.; Bunning, T. J.; White, T. J. Autonomous, Hands-Free Shape Memory in Glassy, Liquid Crystalline Polymer Networks. *Adv. Mater.* 2012, 24, 2839-2843.
- (8) Liu, Y.; Boyles, J. K.; Genzer, J.; Dickey, M. D. Self-Folding of Polymer Sheets Using Local Light Absorption. *Soft Matter* 2012, 8, 1764-1769.
- (9) Koerner H.; Strong R J.; Smith M L.; Wang D H.; Tan L S.; Lee K M.; White T J.; Vaia R A. Polymer design for high temperature shape memory: Low crosslink density polyimides. *Polymer*, 2013, 54, 391-402.
- (10) Lendlein, A.; Jiang, H. Y.; Junger, O.; Langer, R. Light-Induced Shape-Memory Polymers. *Nature* 2005, 434, 879-882.
- (11) Zhang, X. Z.; Zhou, Q. Q.; Liu, H. R.; Liu, H. W. Uv Light Induced Plasticization and Light Activated Shape Memory of Spiropyran Doped Ethylene-Vinyl Acetate Copolymers. *Soft Matter* 2014, 10, 3748-3754.
- (12) Zhang, H. J.; Xia, H. S.; Zhao, Y. Light-Controlled Complex Deformation and Motion of Shape-Memory Polymers Using a Temperature Gradient. *ACS Macro Lett.* 2014, 3, 940-943.
- (13) Zhang, H. J.; Xia, H. S.; Zhao, Y. Optically Triggered and Spatially Controllable Shape-Memory Polymer-Gold Nanoparticle Composite Materials. *J. Mater. Chem.* 2012, 22, 845-849.
- (14) Leng, J. S.; Lan, X.; Liu, Y. J.; Du, S. Y.; Huang, W. M.; Liu, N.; Phee, S. J.; Yuan, Q. Electrical Conductivity of Thermoresponsive Shape-Memory Polymer with Embedded Micron Sized Ni Powder Chains. *Appl. Phys. Lett.* 2008, 92.
- (15) Luo, X. F.; Mather, P. T. Conductive Shape Memory Nanocomposites for High Speed Electrical Actuation. *Soft Matter* 2010, 6, 2146-2149.
- (16) Mohr, R.; Kratz, K.; Weigel, T.; Lucka-Gabor, M.; Moneke, M.; Lendlein, A. Initiation of Shape-Memory Effect by Inductive Heating of Magnetic Nanoparticles in Thermoplastic Polymers. *Proceedings of the National Academy of Sciences of the United States of America* 2006, 103, 3540-3545.

- (17) Huang, W. M.; Yang, B.; An, L.; Li, C.; Chan, Y. S. Water-Driven Programmable Polyurethane Shape Memory Polymer: Demonstration and Mechanism. *Appl. Phys. Lett.* 2005, 86.
- (18) Yang, B.; Huang, W. M.; Li, C.; Li, L. Effects of Moisture on the Thermomechanical Properties of a Polyurethane Shape Memory Polymer. *Polymer* 2006, 47, 1348-1356.
- (19) He, Z.; Satarkar, N.; Xie, T.; Cheng, Y.-T.; Hilt, J. Z. Remote Controlled Multishape Polymer Nanocomposites with Selective Radiofrequency Actuations. *Adv. Mater.* 2011, 23, 3192-3196.
- (20) Xie, T.; Rousseau, I. A. Facile Tailoring of Thermal Transition Temperatures of Epoxy Shape Memory Polymers. *Polymer* 2009, 50, 1852-1856.
- (21) Lendlein, A.; Langer, R. Biodegradable, Elastic Shape-Memory Polymers for Potential Biomedical Applications. *Science* 2002, 296, 1673-1676.
- (22) El Feninat, F.; Laroche, G.; Fiset, M.; Mantovani, D. Shape Memory Materials for Biomedical Applications. *Adv. Eng. Mater.* 2002, 4, 91-104.
- (23) Gall, K.; Yakacki, C. M.; Liu, Y. P.; Shandas, R.; Willett, N.; Anseth, K. S. Thermomechanics of the Shape Memory Effect in Polymers for Biomedical Applications. *J. Biomed. Mater. Res.* 2005, 73A, 339-348.
- (24) Chen, C. M.; Chiang, C. L.; Lai, C. L.; Xie, T.; Yang, S. Buckling-Based Strong Dry Adhesives Via Interlocking. *Adv. Funct. Mater.* 2013, 23, 3813-3823.
- (25) Eisenhaure, J. D.; Xie, T.; Varghese, S.; Kim, S. Microstructured Shape Memory Polymer Surfaces with Reversible Dry Adhesion. *ACS Appl. Mater. Interfaces* 2013, 5, 7714-7717.
- (26) Xie, T.; Xiao, X. C. Self-Peeling Reversible Dry Adhesive System. *Chem. Mater.* 2008, 20, 2866-2868.
- (27) Xu, H. X.; Yu, C. J.; Wang, S. D.; Malyarchuk, V.; Xie, T.; Rogers, J. A. Deformable, Programmable, and Shape-Memorizing Micro-Optics. *Adv. Funct. Mater.* 2013, 23, 3299-3306.
- (28) Chen, C. M.; Reed, J. C.; Yang, S. Guided Wrinkling in Swollen, Pre-Patterned Photoresist Thin Films with a Crosslinking Gradient. *Soft Matter* 2013, 9, 11007-11013.
- (29) Luo, Y.; Guo, Y.; Gao, X.; Li, B.-G.; Xie, T. A General Approach Towards Thermoplastic Multishape-Memory Polymers Via Sequence Structure Design. *Adv. Mater.* 2013, 25, 743-748.
- (30) Kelch, S.; Choi, N. Y.; Wang, Z. G.; Lendlein, A. Amorphous, Elastic Ab Copolymer Networks from Acrylates and Poly (L-Lactide)-Ran-Glycolide Dimethacrylates. *Adv. Eng. Mater.* 2008, 10, 494-502.
- (31) Voit, W.; Ware, T.; Dasari, R. R.; Smith, P.; Danz, L.; Simon, D.; Barlow, S.; Marder, S. R.; Gall, K. High-Strain Shape-Memory Polymers. *Adv. Funct. Mater.* 2010, 20, 162-171.
- (32) Yakacki, C. M.; Shandas, R.; Safranski, D.; Ortega, A. M.; Sassaman, K.; Gall, K. Strong, Tailored, Biocompatible Shape-Memory Polymer Networks. *Adv. Funct. Mater.* 2008, 18, 2428-2435.
- (33) Nair, D. P.; Cramer, N. B.; Scott, T. F.; Bowman, C. N.; Shandas, R.

- Photopolymerized Thiol-Ene Systems as Shape Memory Polymers. *Polymer* 2010, 51, 4383-4389.
- (34) Senyurt, A. F.; Hoyle, C. E.; Wei, H. Y.; Piland, S. G.; Gould, T. E. Thermal and Mechanical Properties of Cross-Linked Photopolymers Based on Multifunctional Thiol-Urethane Ene Monomers. *Macromolecules* 2007, 40, 3174-3182.
- (35) Rousseau, I. A.; Xie, T. Shape Memory Epoxy: Composition, Structure, Properties and Shape Memory Performances. *J. Mater. Chem.* 2010, 20, 3431-3441.
- (36) Feldkamp, D. M.; Rousseau, I. A. Effect of the Deformation Temperature on the Shape-Memory Behavior of Epoxy Networks. *Macromol. Mater. Eng.* 2010, 295, 726-734.
- (37) Jing, X. H.; Liu, Y. Y.; Liu, Y. X.; Liu, Z. G.; Tan, H. F. Toughening-Modified Epoxy-Amine System: Cure Kinetics, Mechanical Behavior, and Shape Memory Performances. *J. Appl. Polym. Sci.* 2014, 131.
- (38) Leng, J. S.; Wu, X. L.; Liu, Y. J. Effect of a Linear Monomer on the Thermomechanical Properties of Epoxy Shape-Memory Polymer. *Smart Mater. Struct.* 2009, 18(9), 095031.
- (39) Leonardi, A. B.; Fasce, L. A.; Zucchi, I. A.; Hoppe, C. E.; Soule, E. R.; Perez, C. J.; Williams, R. J. J. Shape Memory Epoxies Based on Networks with Chemical and Physical Crosslinks. *Eur. Polym. J.* 2011, 47, 362-369.
- (40) Liu, Y. Y.; Han, C. M.; Tan, H. F.; Du, X. W. Thermal, Mechanical and Shape Memory Properties of Shape Memory Epoxy Resin. *Mater. Sci. Eng. A* 2010, 527, 2510-2514.
- (41) Biju, R.; Gouri, C.; Nair, C. P. R. Shape Memory Polymers Based on Cyanate Ester-Epoxy-Poly (Tetramethyleneoxide) Co-Reacted System. *Eur. Polym. J.* 2012, 48, 499-511.
- (42) Wu, X. L.; Kang, S. F.; Xu, X. J.; Xiao, F.; Ge, X. L. Effect of the Crosslinking Density and Programming Temperature on the Shape Fixity and Shape Recovery in Epoxy-Anhydride Shape-Memory Polymers. *J. Appl. Polym. Sci.* 2014, 131.
- (43) Wang, R. M.; Xiao, X. C.; Xie, T. Viscoelastic Behavior and Force Nature of Thermo-Reversible Epoxy Dry Adhesives. *Macromol. Rapid Commun.* 2010, 31, 295-299.
- (44) Park, J. H.; Jana, S. C. Mechanism of Exfoliation of Nanoclay Particles in Epoxy-Clay Nanocomposites. *Macromolecules* 2003, 36, 2758-2768.
- (45) Luo, X.; Mather, P. T. Shape Memory Assisted Self-Healing Coating. *ACS Macro Lett.* 2013, 2, 152-156.
- (46) Xiao X.; Xie T.; Cheng Y T. Self-healable graphene polymer composites. *J. Mater. Chem.* 2010, 20, 3508-3514.
- (47) Luo, X.; Mather, P. T. Triple-Shape Polymeric Composites (Tspcs). *Adv. Funct. Mater.* 2010, 20, 2649-2656.
- (48) Xie, T.; Xiao, X. Cheng, Y. T. Achieving triple-shape memory effect in polymer bilayers. *Macromol. Rapid Commun.* 2009, 30, 1823-1827.
- (49) Yakacki C M.; Willis S.; Luders C.; Gall, K. Deformation Limits in Shape - Memory Polymers. *Adv. Eng. Mater.* 2008, 10, 112-119.
- (50) Horie, K.; Hiura, H.; Sawada, M.; Mita, I.; Kambe, H. Calorimetric Investigation

of Polymerization Reactions .3. Curing Reaction of Epoxides with Amines. J. Polym. Sci. Pol. Chem. 1970, 8, 1357-1372.

(51) Miller, D. R.; Macosko, C. W. Substitution Effects in Property Relations for Stepwise Polyfunctional Polymerization. Macromol. 1980, 13, 1063-1069.

(52) Matejka, L. Amine Cured Epoxide Networks: Formation, Structure, and Properties. Macromol. 2000, 33, 3611-3619.

Table of Contents

High Strain Epoxy Shape Memory Polymer

Ning Zheng, Guangqiang Fang, Zhengli Cao, Qian Zhao, Tao Xie

